Chemical Engineering Science 287 (2024) 119662

Contents lists available at ScienceDirect

Chemical Engineering Science

journal homepage: www.elsevier.com/locate/ces

Iterative real-time optimization of a reductive amination process in a thermomorphic multiphase system

Anwesh Reddy Gottu Mukkula [a,*], Tim Benjamin Riemer [b], Alexander Kühl [b], Dieter Vogt [b], Sebastian Engell [a]

[a] Process Dynamics and Operations Group, Technische Universität Dortmund, 44221 Dortmund, Germany
[b] Laboratory of Industrial Chemistry, Technische Universität Dortmund, 44221 Dortmund, Germany

ARTICLE INFO

Keywords:
Iterative real-time optimization
Model adequacy
Modifier adaptation
Process optimization
Reductive amination

ABSTRACT

In this paper, we discuss the optimization of the operation of a reductive amination (RA) reaction process in a miniplant without an accurate process model using iterative real-time optimization (RTO). The rhodium-catalyzed RA of undecanal with diethylamine produces a tertiary amine from a long-chain aldehyde and is performed in a thermomorphic multiphase system (TMS) to recover and reuse the expensive catalyst efficiently. An iterative RTO method called modifier adaptation with quadratic approximation (MAWQA) is used in combination with guaranteed model adequacy (GMA) to drive the RA process to its optimum iteratively. MAWQA utilizes online measurements to overcome model deficiencies. GMA ensures that the model used in MAWQA satisfies the model adequacy conditions. The optimal operating conditions of the RA process in the miniplant were identified during an experimental run of the plant, thereby validating the applicability and efficiency of MAWQA with GMA. The results illustrate the benefits of process optimization using iterative RTO methods without accurate process models.

1. Introduction

Reductive amination (RA) is an effective method for producing alkyl amines that are important intermediates for synthesizing pharmaceuticals (Afanasyev et al., 2019), materials and surfactants (Strohmann et al., 2022). Starting from a carbonyl compound, the desired amines are formed, with water as the only by-product. The first step is the condensation of an aldehyde or ketone with the substrate amine (ammonia, primary or secondary amine) to the respective imine or enamine, which is then hydrogenated to the final primary, secondary or tertiary amine. Hydrogenation occurs catalytically with molecular hydrogen, which is accessible sustainably via electrolysis. RA has already been intensively researched in the academic and industrial sectors (Bianga et al., 2020a; Künnemann et al., 2020; Kirschtowski et al., 2020, 2021; Jameel and Stein, 2022; Weber et al., 2021; Hahn et al., 2019; Jagadeesh et al., 2017) and was first reported by Mignonac (1921) in the year 1921. Most industrial amination processes are heterogeneously catalyzed (Hayes, 2001). This allows easy separation and recycling of the catalyst and makes it possible to reach low limits of catalyst concentration in the final products, which often must be met (Gürsel et al., 2015). However, if high selectivities and mild reaction conditions are required, or if chiral amines are to be produced, homogeneous transition metal catalysis often is the more efficient tool (Reshi et al., 2021). To still enable the separation and recycling of the dissolved catalyst, thermomorphic multiphase systems offer an elegant solution by exploiting the temperature dependency of the miscibility gap. The reaction takes place under monophasic conditions, and after the reaction, the mixture is cooled down and split into two phases. Ideally, one phase contains the product, while the homogenous catalyst remains in the other phase, enabling easy separation by decantation (Bianga et al., 2019).

To achieve a short time-to-market for modified or new products, carrying out the process development already with the assistance of model-based real-time optimization on the miniplant scale is worthwhile. The best possible performance of a process can then be determined already during the process development phase, thus providing a reliable basis for its evaluation and for further decisions in the design process. Additionally, the developed schemes can serve as the basis for the development of the automation systems of the real plant and hence speed up the detailed design and commissioning phase (Engell, 2022). The goal of this work was to identify the optimal operating conditions

* Corresponding author.
E-mail address: anweshreddy.gottumukkula@tu-dortmund.de (A.R. Gottu Mukkula).

https://doi.org/10.1016/j.ces.2023.119662
Received 14 August 2023; Received in revised form 13 November 2023; Accepted 19 December 2023
Available online 2 January 2024

of the RA reaction in the miniplant, which will be referred to as the RA-process in this paper, as well as to validate the efficiency and applicability of a specific iterative RTO algorithm, MAWQA with GMA which in this paper is demonstrated for the first time at a real process.

Real-time optimization (RTO) represents the upper-level optimization problem in a hierarchical control structure. RTO provides inputs to the regulatory control layer and helps to optimally implement the decisions which are generated by the planning & scheduling layer (Darby et al., 2011; Engell, 2007). Classically in the optimization problem a rigorous steady-state process model is employed where the objective and constraint functions are formulated based on the information from the planning & scheduling layer, and the optimum from the RTO layer is passed on to the underlying regulatory control layer as set-points. When an accurate process model is available, one can compute the optimum operating parameters by formulating and solving this model-based optimization problem. However, for complex multiphase processes, e.g. the RA-process, significant uncertainties exist in the process model. Therefore it is challenging to identify the optimal operating conditions. Classically this is done by experiments on the miniplant or pilot scale, following fixed experimental designs. With this approach, a large number of experiments are needed to identify the optimal conditions precisely. Therefore we propose to use a combination of model-based and data-based optimization to find the optimal conditions fast and reliably. Moreover, the experimental identification can only be done for a limited set of intended operational regimes (e.g. throughputs, product qualities) while an automatic on-line identification will adapt to new demands from the upper layer.

The uncertainty in a process model can be parametric or structural, or both. Parametric uncertainty in a process model means that the model parameters are not accurately known. Structural uncertainty in a process model occurs if some phenomena that are occurring in the process are described in a simplified form, or ignored. Iterative real-time optimization (RTO) methods can overcome uncertainties and identify the process optimum despite the fact that the model is inaccurate. The two-step approach was proposed in Jang et al. (1987), and later refined in Chen and Joseph (1987), to overcome parametric model uncertainties by iteratively correcting the model parameters using process measurements and then re-optimizing the process using the corrected model. However the two-step approach cannot handle structural model uncertainties systematically and can even lead to worse results than not adapting the parameters (Chachuat et al., 2008). The integrated system optimization and parameter estimation (ISOPE) approach proposed in Roberts (1979) handles both parametric- and structural model uncertainties. It iteratively modifies the objective function of the model-based optimization problem in addition to correcting the model parameters. It was shown in Tatjewski (2002); Brdyś and Tatjewski (2005) that both parametric- and structural model uncertainties can indeed be handled by only iteratively modifying the objective function without the need for updating the model parameters. The approach in Tatjewski (2002) was extended in Gao and Engell (2005) modifying also the constraints of the model-based optimization problem, which in Gao and Engell (2005) was called iterative gradient-modification optimization (IGMO). In Marchetti et al. (2009), the IGMO approach was analyzed in depth and called modifier adaptation (MA).

The model-based optimization problem in ISOPE, IGMO or MA is modified using steady-state process measurements. From these measurements, the gradients of the objective function and of the constraints are estimated for the real plant, as well as the mismatch of the constraints. It is critical for the approach to approximate the process gradients accurately as they are vital to identify a process optimum. To ensure a reliable approximation of process gradients, it was proposed in Gao et al. (2016) to use quadratic approximation (QA) of the response functions of the real plant for process gradient estimation and the resulting algorithm was called modifier adaptation with quadratic approximation (MAWQA). In ISOPE, MA, and MAWQA, it is a prerequisite for the successful application of the algorithms that the available process model satisfies the so-called model adequacy conditions (Marchetti et al., 2009, 2016; Gao et al., 2015; Forbes and Marlin, 1996; Bonvin and Srinivasan, 2013). For a process model to be adequate it is required that the Lagrangian of the modified optimization problem satisfies the necessary second-order conditions in addition to the KKT conditions at the true (but unknown) plant optimum. If this is not the case, the method does not converge but oscillates between different solutions. In Faulwasser and Bonvin (2014) it was proposed to use second-order correction terms in the MA context to match the Hessian of the process. However, accurately estimating the Hessian from observed data is challenging and hardly practical. Another possibility to handle the issue is convex model approximation of the objective and constraint functions as proposed in François and Bonvin (2013), which however may slow down the rate of convergence to the optimum. The issue of model adequacy was handled in Ahmad et al. (2019) by updating the model parameters iteratively while imposing the adequacy conditions at the current steady state. Convexity is not imposed, which may improve the speed of convergence. Recently in Gottu Mukkula and Engell (2020), the guaranteed model adequacy (GMA) approach was proposed to handle the process model inadequacy issue in MAWQA. Here, quadratic approximations of the objective and constraint functions are employed.

Besides the two-step approach and MA-based methods, also the extremum seeking control (ESC) (Krstić and Wang, 2000), necessary conditions of optimality (NCO)-tracking, and self-optimizing control (SOC) (Jäschke and Skogestad, 2011) schemes address the issue of the presence of unknown or imprecise process models. A comprehensive survey of the existing iterative RTO schemes can be found in Marchetti et al. (2016). However, despite a large body of theoretical work, the number of experimental evaluations of iterative RTO is small (Marchetti et al., 2020; Hernandez et al., 2018; Gottu Mukkula et al., 2020b,a; Navia et al., 2017). MAWQA was before used for the optimization of real processes in Hernandez et al. (2018); Gottu Mukkula et al. (2020b,a). In Hernandez et al. (2018), hydroformylation of 1-dodecene to tridecanal performed in a thermomorphic multiphase system (TMS) with the solvents n-decane and DMF was optimized using MAWQA but without GMA.

In this contribution, the operation of a RA process in a miniplant is optimized during an experimental run despite plant-model mismatch using the recently reported MAWQA with GMA approach (Gottu Mukkula and Engell, 2020) due to its capability to handle plant-model mismatch, model inadequacy, measurement noise, and gradient approximation without additional input perturbations. To the authors' knowledge, this is the first practical application of MAWQA with GMA. The inclusion of GMA avoids undesired input oscillations and enabled MAWQA to converge smoothly to the optimum. In the following sections, we present the RA process in the miniplant, the iterative RTO method MAWQA with GMA, the optimization goal, and the experimental results.

2. Process description

In this work, the reductive amination of undecanal, a C–11 aldehyde, by homogenously catalyzed addition of diethylamine (DEA) in a miniplant (Künnemann et al., 2020) is investigated. For a high activity and selectivity to the desired tertiary amine, a catalyst system consisting of Rh(acac)cod and the bidentate ligand Sulfoxantphos was chosen (Bianga et al., 2020a,b). The reaction scheme of the RA of undecanal illustrated in Fig. 1, is thermoneutral according to Kirschtowski et al. (2021). The first reaction step is the condensation of undecanal and DEA to N,N-diethylundecylenamine. The enamine then reacts further to the desired product, N,N-diethylundecylamine. Besides the hydrogenation of the enamine, the aldehyde can also be hydrogenated to the alcohol, i.e. undecanol. To suppress the hydrogenation to the alcohol, carbon monoxide (CO) is continuously dosed into the hydrogen gas phase during the miniplant operation. Its presence proved to be the most effective method for reducing alcohol formation in previous investigations of the

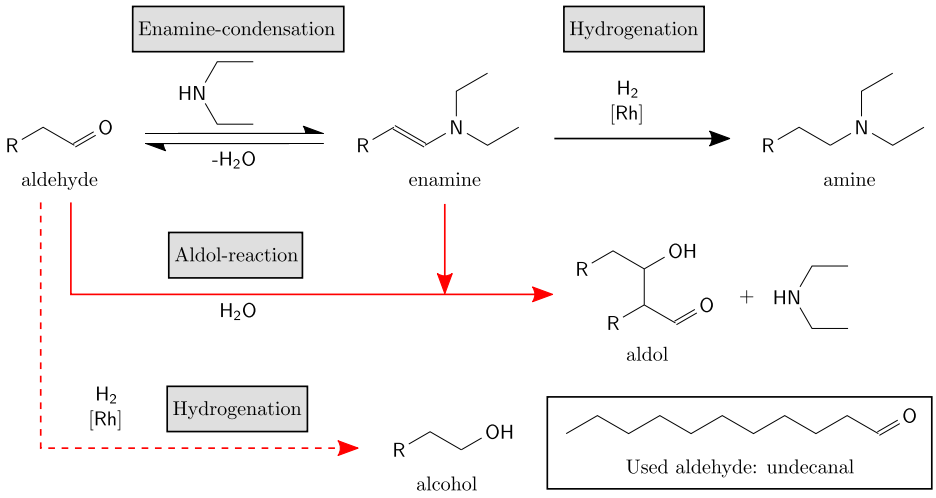

Fig. 1. Reaction scheme for the reductive amination of undecanal with diethylamine.

same catalyst system (Weber et al., 2021). Furthermore, the concentration of undecanal should be kept low by shifting the equilibrium to the enamine through an excess of DEA and a low water concentration. In addition, fast hydrogenation of the enamine to the tertiary amine is desirable to constantly remove enamine from the reaction equilibrium of the condensation. Another side reaction is the aldol reaction, which is catalyzed by the intermediate enamine, which reacts with another aldehyde molecule to form the by-product aldol, releasing diethylamine. With an increase in the reaction temperature, the speed of the competing reaction does not increase as fast as that of the primary reaction. This side reaction can also be inhibited by a rapid hydrogenation of the enamine.

The reductive amination reaction is performed in a thermomorphic multiphase system (TMS) to ensure the efficient recovery of the catalyst and the separation of the product (Künnemann et al., 2020; Bianga et al., 2019). At high temperatures, used in the reactor, the solvents are completely miscible, and at low temperatures, used in the downstream separation step, a phase separation occurs. Polar and non-polar solvents are chosen such that after cooling, the non-polar product remains in the non-polar solvent phase, whereas the active homogeneous catalyst dissolves in the polar solvent phase and can be efficiently recycled. For efficient catalyst recovery, the solubility of the catalyst has to be significantly higher in the polar solvent than in the non-polar solvent. Based on the results in Kirschtowski et al. (2020), dodecane and methanol are used as non-polar and polar solvents for the RA reaction in the miniplant.

The process flow diagram of the RA-process and a picture of the miniplant are shown in Figs. 2 and 3, respectively. The liquid reactants for the reductive amination reaction are fed continuously into the CSTR from three feed tanks. Feed tank B1 contains undecanal in dodecane, feed tank B2 contains catalyst in methanol, and feed tank B3 contains DEA. Hydrogen and CO are fed into the CSTR such that a ratio of 1:9 of CO to hydrogen is maintained in the reactor. The CSTR is jacketed and heated using an oil bath. The RA reaction is performed at a constant pressure of 30 bar and at temperatures higher than 90 °C. Under these conditions, the reaction mixture is monophasic, favoring the reaction without transport limitation (Huxoll et al., 2022; Kirschtowski et al., 2020). The reaction mixture from the outlet of the CSTR is cooled down and transferred to the decanter. The temperature of the decanter is maintained at 5 °C, at which a miscibility gap exists (Huxoll et al., 2022), causing the reaction mixture to separate into polar and non-polar phases. The non-polar phase containing the desired product is depressurized in a flash vessel and then collected in the product tank. The polar phase containing the catalyst is recycled back into the CSTR. Losses of methanol and catalyst via the product stream are compensated by adding a makeup stream via the pump P2. The water produced during the enamine-condensation remains in the polar phase, therefore it continuously accumulates during the process. The water accumulation can be avoided by adding another unit operation, e.g. a membrane separation unit as presented in Schlüter et al. (2021). However, this is not within the scope of this work. In Schlüter et al. (2021) the water-tolerance in the hydroaminomethylation of 1-decene with diethylamine was determined for the phase ratios (polar to non-polar) of 1:1 and 4:1 at 125 °C to be 6 and 13 wt%, respectively. Based on the results presented in Schlüter et al. (2021), the water tolerance limit in the RA-process for a 3 : 1 phase ratio at 125 °C is estimated as 12 wt%, above this value a biphasic mixture forms, hindering the reaction due to liquid-liquid mass-transfer limitations.

3. Formulation of the optimization problem

The goal is to identify the optimal values for the residence time (throughput) and the reaction temperature such that the amount of the amine ($\dot{n}_{prod,Amine}$) produced per unit time is maximized. The residence time of the reactor is manipulated by varying the total volumetric feed rate of the liquid reactants entering the reactor ($\dot{V}_{in}$), and the reactor temperature (T_R) is controlled by manipulating the temperature of the oil bath.

The nominally optimal inputs of the process can be obtained by solving the following nominal model-based nonlinear optimization problem:

$$\boldsymbol{u}_m^* = \arg \max_{\boldsymbol{u}\in[\boldsymbol{u}^L,\boldsymbol{u}^U]} J(\hat{\boldsymbol{y}},\boldsymbol{u}) \tag{1a}$$

$$\text{s.t. } \hat{\boldsymbol{y}} = \boldsymbol{F}_m(\boldsymbol{u}), \tag{1b}$$

$$\boldsymbol{G}(\hat{\boldsymbol{y}},\boldsymbol{u}) \le \boldsymbol{0}, \tag{1c}$$

where the objective function is $J(\hat{\boldsymbol{y}},\boldsymbol{u}) := \dot{n}_{prod,Amine}$, the manipulated variables are $\boldsymbol{u} := [T_R, \dot{V}_{in}]^T$ with $\boldsymbol{u}^L$ and $\boldsymbol{u}^U$ as their lower and upper limits. The optimization problem is constrained by a nominal steady-state process model (1b) which here is represented by a function $\boldsymbol{F}_m : \mathbb{R}^{n_u} \to \mathbb{R}^{n_y}$ which maps n_u model inputs to n_y output variables. In addition to the nominal process model, there also can be process constraints (1c) which here are represented by the function $\boldsymbol{G} : \mathbb{R}^{n_u} \times \mathbb{R}^{n_y} \to \mathbb{R}^{n_c}$, in which n_c is the number of constraints. However, the RA-process is unconstrained besides the bounds on the input variables. The accuracy of the process model directly affects the possibility of identifying the optimum of the real process $\boldsymbol{u}_p^*$. Oversimplification in modelling, incomplete process understanding, or inadequate parameter estimation lead to a mismatch between the nominal model (1b)

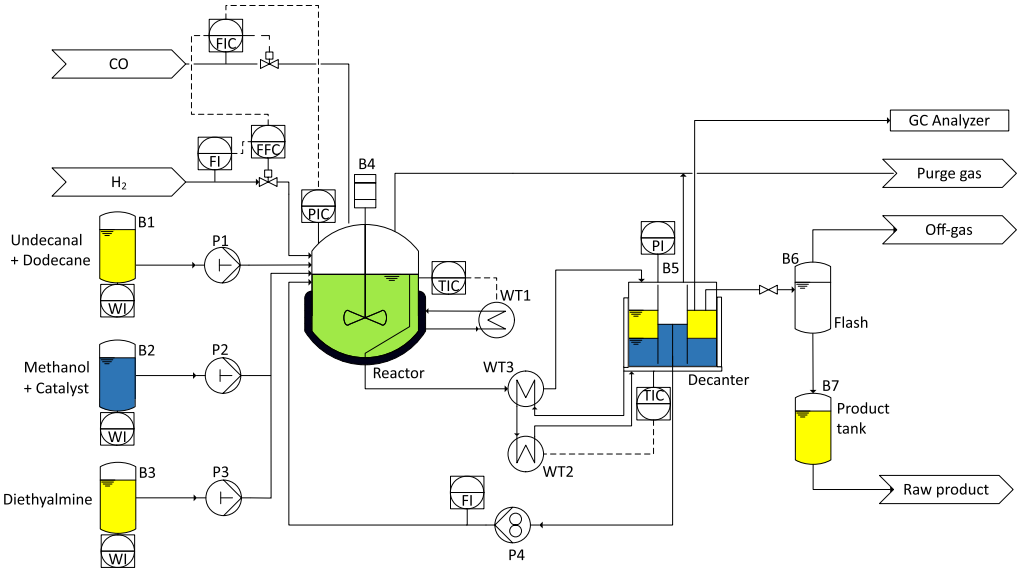

Fig. 2. Process flow diagram of the reductive amination process. Yellow and blue colours represent non-polar and polar phases, respectively. Green colour represents a homogeneous liquid phase.

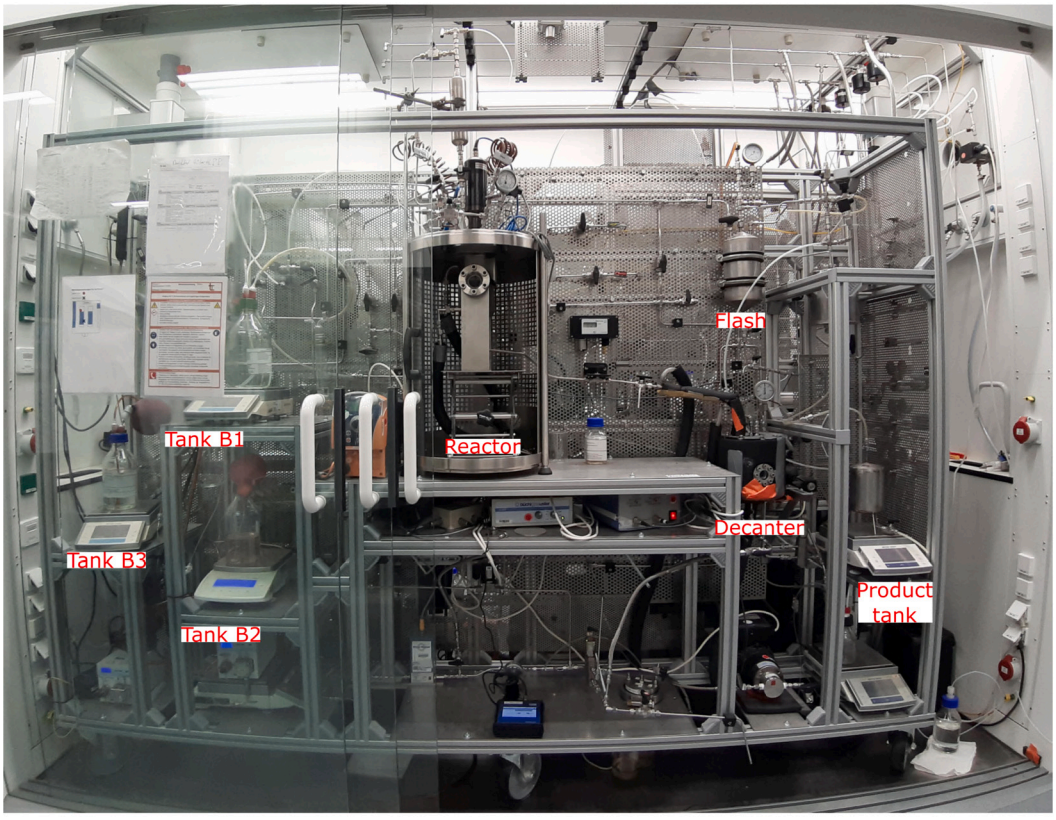

Fig. 3. Photograph of the miniplant in which the reductive amination of undecanal was performed.

and the unknown real process behaviour denoted as $\boldsymbol{y}_p = \boldsymbol{F}_p(\boldsymbol{u})$. Therefore, in the presence of a plant-model mismatch, the solution of (1) will not match the optimum of the real process. Therefore, the iterative real-time optimization method MAWQA with GMA is used to identify the real optimum during operation of the miniplant despite the plant-model mismatch. In the following subsection, the key aspects of MAWQA with GMA are presented.

3.1. Modifier adaptation with quadratic approximation

MAWQA is a MA-based iterative RTO method that embodies elements from derivative-free optimization (DFO) (Gao et al., 2015, 2016). In MA, the nominal model-based optimization problem (1) is iteratively modified and solved until the solution converges to the real process optimum (Gao and Engell, 2005; Marchetti et al., 2009). The objective

function (1a) and the constraint functions (1c) in the model-based optimization problem (1) are modified by bias and gradient correction terms. The modified model-based optimization problem, i.e., the MA problem, in the k^{th} iteration is:

$$\hat{\boldsymbol{u}}^{k+1} = \arg \min_{\boldsymbol{u}\in[\boldsymbol{u}^L,\boldsymbol{u}^U]} J_m^{ad,k}(\hat{\boldsymbol{y}},\boldsymbol{u}) \tag{2a}$$

$$\text{s.t. } \hat{\boldsymbol{y}} = \boldsymbol{F}_m(\boldsymbol{u}), \tag{2b}$$

$$\boldsymbol{G}_m^{ad,k}(\hat{\boldsymbol{y}},\boldsymbol{u}) \le \boldsymbol{0}. \tag{2c}$$

The modified objective and constrained functions in the k^{th} iteration of the MA problem are defined as:

$$J_m^{ad,k}(\hat{\boldsymbol{y}},\boldsymbol{u}) := J(\hat{\boldsymbol{y}},\boldsymbol{u}) + (J(\boldsymbol{y}_p^k,\boldsymbol{u}^k) - J(\hat{\boldsymbol{y}}^k,\boldsymbol{u}^k)) + (\nabla J(\boldsymbol{y}_p^k,\boldsymbol{u}^k) - \nabla J(\hat{\boldsymbol{y}}^k,\boldsymbol{u}^k))^T(\boldsymbol{u}-\boldsymbol{u}^k), \tag{3a}$$

$$\boldsymbol{G}_m^{ad,k}(\hat{\boldsymbol{y}},\boldsymbol{u}) := \boldsymbol{G}(\hat{\boldsymbol{y}},\boldsymbol{u}) + (\boldsymbol{G}(\boldsymbol{y}_p^k,\boldsymbol{u}^k) - \boldsymbol{G}(\hat{\boldsymbol{y}}^k,\boldsymbol{u}^k)) + (\nabla \boldsymbol{G}(\boldsymbol{y}_p^k,\boldsymbol{u}^k) - \nabla \boldsymbol{G}(\hat{\boldsymbol{y}}^k,\boldsymbol{u}^k))^T(\boldsymbol{u}-\boldsymbol{u}^k), \tag{3b}$$

where $\nabla J(\hat{\boldsymbol{y}}^k,\boldsymbol{u}^k)$ and $\nabla \boldsymbol{G}(\hat{\boldsymbol{y}}^k,\boldsymbol{u}^k)$ represent the nominal model gradients, i.e., the gradients of J and $\boldsymbol{G}$ w.r.t. $\boldsymbol{u}$ evaluated for the inputs $\boldsymbol{u}^k$. The terms $J(\boldsymbol{y}_p^k,\boldsymbol{u}^k)$ and $\boldsymbol{G}(\boldsymbol{y}_p^k,\boldsymbol{u}^k)$ represent the objective and constraint functions of the real process, which are computed from the inputs $\boldsymbol{u}^k$ and the corresponding steady-state plant measurements $\boldsymbol{y}_p^k$. $\nabla J(\boldsymbol{y}_p^k,\boldsymbol{u}^k)$ and $\nabla \boldsymbol{G}(\boldsymbol{y}_p^k,\boldsymbol{u}^k)$ are the gradients of the response of the real process w.r.t. $\boldsymbol{u}$ evaluated for the inputs $\boldsymbol{u}^k$ and corresponding steady-state process measurements $\boldsymbol{y}_p^k$. Upon convergence, the optimum of the MA problem satisfies the optimality conditions of the real process (Marchetti et al., 2016). If the iterative procedure converges to a stationary solution, this is the real (local) process optimum within the domain of attraction of this optimum.

The gradients of the real process objective and constraint functions play a critical role in the success of MA. As they usually cannot be measured, they must be approximated using process measurements. Finite differences or Broyden's formula (Roberts, 2000) are often used for gradient approximation (Gao et al., 2016; Marchetti et al., 2016). However, they are susceptible to measurement noise. To obtain reliable estimates, additional process perturbations may be needed (Gao and Engell, 2005).

In MAWQA, elements from derivative-free optimization (DFO) are combined with MA to overcome the issues in gradient approximation. In MAWQA, a quadratic approximation function Q defined as

$$Q(c_0,\boldsymbol{c},\mathbb{H};\boldsymbol{u}) = c_0 + \boldsymbol{c}^T\boldsymbol{u} + \frac{1}{2}\boldsymbol{u}^T\mathbb{H}\boldsymbol{u} \tag{4}$$

is fitted to the observed steady-state values of the cost function and of the constraint functions to estimate the gradients. The QA smooths the measurement noise and does not require additional process perturbations after enough data has been collected (Gao et al., 2015; Wenzel et al., 2015). The parameters of the QA function, $c_0, \boldsymbol{c}$ and $\mathbb{H}$ can be estimated once there are process measurements for at least $\frac{(n_u+1)(n_u+2)}{2}$ different input points. The parameter $\mathbb{H}$ represents a $n_u \times n_u$ dimensional symmetric matrix, which is the Hessian of the QA function. After fitting a QA function, the real process gradients are estimated by differentiating the fitted QA function w.r.t. $\boldsymbol{u}$. In MAWQA, a QA function is fitted to the objective function J_Q and to each constraint function G_Q, and the QA function parameters are updated at every iteration. From these parameters, the gradients are computed and inserted into (3b) and then the modified optimization problem (2) is solved.

Instead of solving (2), the QA function-based DFO problem

$$\hat{\boldsymbol{u}}^{k+1} = \arg \min_{\boldsymbol{u}\in[\boldsymbol{u}^L,\boldsymbol{u}^U]} J_Q^k(\boldsymbol{u}) \tag{5a}$$

$$\text{s.t. } \boldsymbol{G}_Q^k(\boldsymbol{u}) \le \boldsymbol{0}, \tag{5b}$$

can be solved instead of the MA problem (2). This is done if in the previous iteration the fitted QA models for the objective and constraint functions are more accurate than the objective and constraint functions of the MA problem. The quality of the models is quantified using the following indicators:

$$\rho_m^k := \max\left\{\left|1 - \frac{J_m^{ad,k} - J_m^{ad,k-1}}{J_p^k - J_p^{k-1}}\right|, \left|1 - \frac{G_{m,1}^{ad,k} - G_{m,1}^{ad,k-1}}{G_{p,1}^k - G_{p,1}^{k-1}}\right|, \ldots, \left|1 - \frac{G_{m,n_c}^{ad,k} - G_{m,n_c}^{ad,k-1}}{G_{p,n_c}^k - G_{p,n_c}^{k-1}}\right|\right\} \tag{6a}$$

$$\rho_Q^k := \max\left\{\left|1 - \frac{J_Q^k - J_Q^{k-1}}{J_p^k - J_p^{k-1}}\right|, \left|1 - \frac{G_{Q,1}^k - G_{Q,1}^{k-1}}{G_{p,1}^k - G_{p,1}^{k-1}}\right|, \ldots, \left|1 - \frac{G_{Q,n_c}^k - G_{Q,n_c}^{k-1}}{G_{p,n_c}^k - G_{p,n_c}^{k-1}}\right|\right\}, \tag{6b}$$

where $J_p^k := J(\boldsymbol{y}_p^k,\boldsymbol{u}^k), G_{p,i=\{1,\ldots,n_c\}}^k := G_{i=\{1,\ldots,n_c\}}(\boldsymbol{y}_p^k,\boldsymbol{u}^k)$. In the k^{th} iteration, the MA problem is solved instead of the QA based problem if $\rho_m^k < \rho_Q^k$ and vice versa. The QA functions are always used either to approximate the process gradients in the MA problem or directly in the QA based optimization problem. A trust region constraint

$$(\boldsymbol{u}-\boldsymbol{u}^k)^T \operatorname{cov}(\mathcal{U}^k)^{-1}(\boldsymbol{u}-\boldsymbol{u}^k) \le \gamma^2, \tag{7}$$

is added as a constraint to the MA problem (2) and to the QA based optimization problem (5) to prevent large input changes as the QA functions are only valid locally. In (7), $\mathcal{U}^k$ represents the set of input data points used for fitting the QA function parameters and γ is a tuning parameter which scales the trust-region. The data points in $\mathcal{U}^k$ consist of so-called neighbourhood points $\mathcal{U}_{nb}^k$ which lie in a close proximity to the input $\boldsymbol{u}^k$ around which the process gradients are approximated, and of the so-called anchor points $\mathcal{U}_{dist}^k$ which are selected to be well distributed around $\boldsymbol{u}^k$. While the anchor points help in determining the shape and orientation of the approximation, the neighbourhood points help to improve the accuracy around $\boldsymbol{u}^k$. In Wenzel et al. (2017) several screening algorithms to identify $\mathcal{U}^k$ were compared. The quality of the distribution of the data points in $\mathcal{U}^k$ is quantified using the condition-number s^k, defined as:

$$\boldsymbol{s}^k = [\boldsymbol{u}^k]^{n_u\times 1} \otimes 1^{\text{cardinality}(\mathcal{U}_{dist}^k)\times 1} - [\mathcal{U}_{dist}^k], \tag{8}$$

where $[\boldsymbol{u}^k], [\mathcal{U}_{dist}^k]$ are matrix representations of $\boldsymbol{u}^k, \mathcal{U}_{dist}^k$. The distribution of the data points is considered ill-conditioned if the inverse of the condition number $\kappa^{-1}(\boldsymbol{s}^k)$ is less than a desired value δ. If $\kappa^{-1}(\boldsymbol{s}^k) < \delta$, additional input perturbations are performed and added to $\mathcal{U}^k$ to improve the distribution of the data points. This condition is referred to as the conditionality-check.

3.2. Guaranteed model adequacy

In modifier adaptation, it is a prerequisite that the nominal-model satisfies the model adequacy condition, i.e., the reduced Hessian of the Lagrangian of the nominal model-based optimization problem at the real process optimum $\boldsymbol{u}_p^*$ is negative definite if the goal is to maximize the objective function and is positive definite if the goal is to minimize the objective function. The Lagrangian of the MA problem in (1) is defined as

$$\mathcal{L}(\hat{\boldsymbol{y}},\boldsymbol{u},\boldsymbol{\mu}) = J(\hat{\boldsymbol{y}},\boldsymbol{u}) + \boldsymbol{\mu}^T\boldsymbol{G}(\hat{\boldsymbol{y}},\boldsymbol{u}), \tag{9}$$

where $\hat{\boldsymbol{y}} = \boldsymbol{F}_m(\boldsymbol{u})$ and $\boldsymbol{\mu}$ is a vector of Lagrange multipliers. However, as the real process optimum $\boldsymbol{u}_p^*$ is not known, it is not possible to evaluate a priori if the nominal-model satisfies the model adequacy condition or not. Additionally, in MAWQA, at some iterations the QA-based optimization problem (5) is solved instead of the MA problem (2) depending

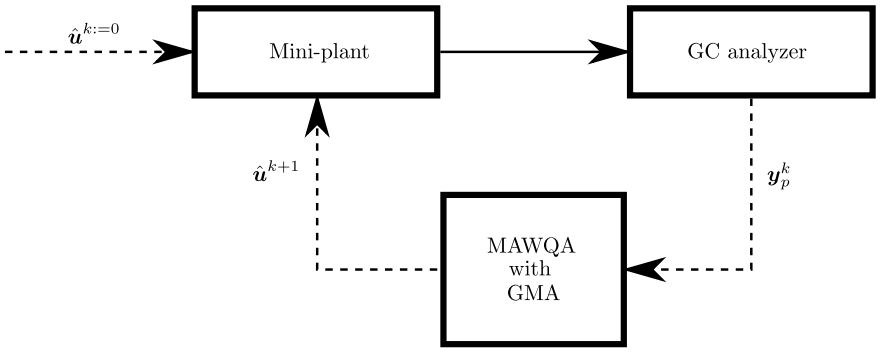

Fig. 4. An illustration of the implementation procedure of iterative-RTO, MAWQA with GMA, to optimize the reductive amination process in the miniplant.

on the quality of the fitted QA models. An inadequate nominal-model leads to unnecessary input moves even after identifying the real process optimum, which is not desired (Gottu Mukkula and Engell, 2020).

In MAWQA with GMA, the issue of model adequacy is addressed by restricting the form of the QA functions. As the Hessian of a QA function $\mathbb{H}$ is independent of the input $\boldsymbol{u}$, the model adequacy condition can be verified a priori. It can be enforced that a QA function is either positive- or negative definite by imposing constraints on $\mathbb{H}$ while fitting the QA functions. GMA addresses the issue of model adequacy in MAWQA in two ways. *First, the objective and the constraint functions of the nominal model-based optimization problem* (1) *are approximated by QA functions offline, and the QA model parameters are selected to satisfy the model adequacy condition.* The nominal model-based optimization problem must be adequate as it defines the Hessian of the MA problem in (2). The fitted objective and constraint functions ensure its adequacy when used in the MA problem (2). *Second, the parameters of the QA models that are built during the iterations of MAWQA for gradient approximation are computed such that the model adequacy condition is satisfied.* These steps ensure that the model adequacy condition is satisfied for all inputs including $\boldsymbol{u}_p^*$. The optimization problem to fit a negative definite QA function to the available m data points is defined as:

$$\min_{c_0,\boldsymbol{c},\mathbb{H}} \sum_{k=1}^{m} \left(J(\boldsymbol{y}_p^k, \boldsymbol{u}^k) - Q(c_0, \boldsymbol{c}, \mathbb{H}; \boldsymbol{u}^k) \right)^2 \tag{10a}$$

$$\text{s.t. } Q(c_0, \boldsymbol{c}, \mathbb{H}; \boldsymbol{u}^k) := c_0 + \boldsymbol{c}^T \boldsymbol{u} + \frac{1}{2} \boldsymbol{u}^T \mathbb{H} \boldsymbol{u} \tag{10b}$$

$$\boldsymbol{u}^T \mathbb{H} \boldsymbol{u} < 0 \quad \forall\, \boldsymbol{u} \in \mathbb{R}^{n_u} \setminus \{0\}, \tag{10c}$$

where $m \geq \frac{(n_u+1)(n_u+2)}{2}$. Selecting the parameters of the QA model to satisfy the model adequacy condition defines a non-convex non-linear optimization problem. In Gottu Mukkula and Engell (2020) it was proposed to use the global quadratic convex estimator (GQCE) from Rosen and Marcia (2004) to identify the QA model parameters. This method is also used here. For a reasonable initial parameter estimate, the algorithm from Rosen and Marcia (2004) almost always converges to a global minimum solution. If a minimum is computed that does not represent the behaviour of the process well, the quality-check in MAWQA, which compares the quality of the fitted QA functions with that of the modified objective and constraint functions in (3), selects the better one for process optimization.

4. Experimental set-up

The RA-process is performed in the miniplant shown in Fig. 3. Before the experiment, tank B1 is filled with a solution of 10 wt% of undecanal in the non-polar solvent dodecane, tank B2 is filled with catalyst dissolved in the polar solvent methanol, and tank B3 is filled with DEA. The reactor is pressurized with CO and hydrogen in a ratio of 1:9. A constant pressure of 30 bar is maintained in the miniplant throughout the experiment. In the reactor, a unimolar ratio of undecanal to DEA is maintained, and the ratio of polar to non-polar solvent of 3:1 is maintained. The temperature in the decanter is set to 5 °C and is maintained constant throughout the experiment. The non-polar phase from the decanter is sampled every hour and is analyzed by gas chromatography (GC), providing the weight fractions of the components undecanal, DEA, product amine, enamine, aldol, undecanol, methanol, dodecane. The recycle stream is sampled offline every four hours to measure the amounts of water, methanol, and DEA. Additionally, the mass flowrate of the product stream is measured using a weight balance. The measurements are used to manipulate the feed flows such that the molar ratios in the reactor are kept at the desired values. The objective function, the molar flowrate of the product $\dot{n}_{prod,Amine}$, is computed from the obtained measurements. The lower and upper bounds of the manipulated variable u_1, the reactor temperature are 363 K and 403 K and of the manipulated variable u_2, the total volumetric inflow into the reactor are 2.75 mL min^{-1} and 5.5 mL min^{-1}, which correspond to a residence time in the reactor between 2 h and 1 h.

4.1. Implementation of MAWQA with GMA

A block diagram of the implementation of MAWQA with GMA at the RA-process is shown in Fig. 4. MAWQA with GMA is initialized with an input $\hat{\boldsymbol{u}}^{k:=0} = [383\,\text{K}, 2.75\,\text{mL min}^{-1}]^T$. The input $\hat{\boldsymbol{u}}^0$ is applied to the RA-process in the miniplant. The non-polar phase in the decanter is sampled hourly to measure the weight fractions of each component. The measurement data $\boldsymbol{y}_p^{k:=0}$ is reconciled (see 4.1.2) and the molar flowrate of amine $\dot{n}_{prod,Amine}$ is passed to the iterative RTO algorithm, MAWQA with GMA. It computes the next input $\hat{\boldsymbol{u}}^{k+1}$ which is then applied to the miniplant. This process is repeated until the input has converged to constant operation conditions which is the real process optimum.

Due to the continuous accumulation of water in the miniplant, the RA process never reaches a steady-state. However, the effect of the accumulation does not reflect in the measurements sampled from the non-polar phase of the decanter if the percentage of water in the reactor, estimated from the percentage of water measured in the recycle stream, is below the water tolerance limit. The RA-process in the miniplant therefore reaches a pseudo steady-state when the measurements from the GC reach a steady-state.

4.1.1. Adequate QA model

In order to obtain an adequate nominal model, the DAE-model presented in the appendix was simulated offline and a negative definite QA model was fitted to the obtained simulation data. For the simulation of the nominal DAE-model, the hydrogenation of aldehyde reaction is suppressed $k_{HYDb,0} := 0$ as no alcohol was observed during the lab experiments. Besides, an additional model error was introduced by assuming a lower amount of the catalyst in the reactor $n_{catalyst} := 4.95 \times 10^{-8}$ than in reality. Additionally, the PC-SAFT model for the LLE in the decanter is approximated using surrogate models. For the nominal-model, the distribution coefficient for water ζ_{H_2O} is set to 1, assuming that all

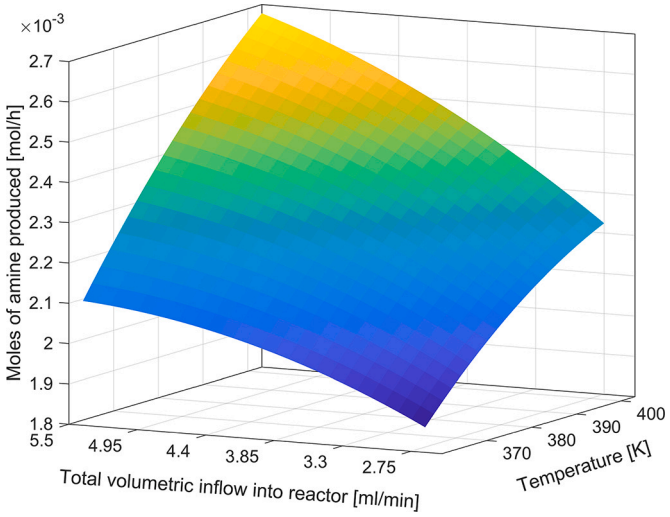

Fig. 5. Surface plot of the QA function fitted to the nominal model to ensure model adequacy.

the water leaves the miniplant via the product stream. Thus there is a significant plant-model mismatch due to the suppression of the hydrogenation reaction, the use of surrogate models for the liquid–liquid separation in the decanter, the assumption that $\zeta_{H_2O} := 1$, and the inaccurate number of moles of catalyst in the reactor. The model parameters of the fitted adequate nominal QA model to compute $\dot{n}_{prod,Amine}$ are

$$c_0 = -0.0154, \tag{11a}$$

$$\boldsymbol{c}^T = [8.3136 \times 10^{-5}, -3.9765 \times 10^{-4}], \tag{11b}$$

$$\mathbb{H} = \begin{bmatrix} -2.0606 \times 10^{-7} & 1.8905 \times 10^{-6} \\ 1.8905 \times 10^{-6} & -4.8324 \times 10^{-5} \end{bmatrix}. \tag{11c}$$

The Hessian matrix $\mathbb{H}$ is negative definite. A response surface plot of the fitted adequate QA model is shown in Fig. 5.

4.1.2. Data reconciliation

The steady-state weight fractions provided by the GC analyzer are reconciled to reduce the effect of measurement errors. For data reconciliation, the Welsch estimator (Korpela et al., 2016; Dennis and Welsch, 1978) is used to compute reconciled plant measurements $\boldsymbol{y}_{p,reconciled}$:

$$\boldsymbol{y}^k_{p,reconciled} = \arg \min_{\boldsymbol{y}_{p,reconciled}} \sum_{i=1}^{n_y} \frac{c_w^2}{2} \left(1 - \exp\left[-\left(\frac{y_{p,reconciled,i} - y_{p,i}(\hat{\boldsymbol{u}}^k)}{c_w} \right)^2 \right] \right) \tag{12a}$$

$$\text{s.t. mass balances of the process are satisfied,} \tag{12b}$$

where $c_w := 2.9846$. The reconciled plant measurements $\boldsymbol{y}^k_{p,reconciled}$ for the input $\hat{\boldsymbol{u}}^k$ are supplied to MAWQA with GMA as steady-state process measurements ($\boldsymbol{y}^k_p := \boldsymbol{y}^k_{p,reconciled}$) to compute the next input $\hat{\boldsymbol{u}}^{k+1}$.

5. Experimental results

Fig. 6 shows the evolution of the manipulated variables over the iterations of the RTO algorithm that result from applying MAWQA with GMA to the RA-process. In the figure, the inputs to the RA-process are represented by red (■) and blue (■) markers for u_1 and u_2. Additional process perturbations that were implemented to compute the gradients are represented by black (□) and magenta (□) markers for u_1 and u_2. The inputs are scaled to lie between 0 and 1, where 0 represents $\boldsymbol{u}^L$ and 1 represents $\boldsymbol{u}^U$, and are plotted using the y-axis on the left. The objective function ($\dot{n}_{prod,Amine}$) for input $\boldsymbol{u}^k$ is represented by blue circles (-○-).

MAWQA with GMA was initialized by applying an initial scaled input $\hat{\boldsymbol{u}}^0 = [0.5, 0]^T$. As not enough data points are available for QA initially, finite differences were used to compute the process gradients. Therefore, after applying $\hat{\boldsymbol{u}}^0$, the miniplant is perturbed twice. The steady-state measurements for the input $\hat{\boldsymbol{u}}^0$ and the two additional perturbations were used to compute the gradients in the first MA optimization. The solution of the MA problem $\hat{\boldsymbol{u}}^1$ was applied to the miniplant. This process was repeated, resulting in the 2nd scaled input $\hat{\boldsymbol{u}}^2 = [0.0125, 0.993]^T$ which was applied to the miniplant. From here on, there are enough data points for QA, and the condition number of the anchor points used for computing the QA was checked in each iteration to ensure a reliable fit. In the 2nd iteration after $\hat{\boldsymbol{u}}^2$, the conditionality of the data points was insufficient and therefore an input represented by black and magenta squares was applied to improve the condition number of the data matrix. QA was performed once the steady-state measurements for the additional perturbation were available. In the 2nd iteration, the quality of the adequate nominal model was superior to the QA model. Therefore the MA based problem formulated using the process gradients approximated from the QA model was solved to compute $\hat{\boldsymbol{u}}^3 = [0.4625, 1]^T$. From the 3rd iteration onwards, the conditionality of the data points was always sufficient and also the quality of the QA model was always superior to the adequate nominal model. Therefore, no additional perturbations were made and always the QA-based optimization problem was solved instead of the MA problem. The input converged to the real process optimum, represented by asterisk [✳,✳], already in the 3rd iteration and remained the same for all future iterations, $\hat{\boldsymbol{u}}^4 = [1, 1]^T$. These steps were all performed automatically by the MAWQA with GMA algorithm without intervention.

Fig. 7 shows the inputs and the dynamic evolution of the RA process in the miniplant over time instead of iterations. The bottom plot in Fig. 7 shows the inputs to the process. The plot in the middle shows the molar flowrate of amine in the product stream, i.e., the objective function. Towards the end of the experiment, as the process stayed close to the optimum steady state, the time between the iterations was longer than in the first iterations. In the top plot, the percentage of water in the reactor is plotted. A vertical dashed-line marks each steady-state of the miniplant. In total, the miniplant was run continuously for approximately 200 hours. During the experiment, the operation was interrupted once, due to the accumulation of water produced in the reaction. The reactor and decanter were emptied and the miniplant was restarted. In line with the predictions of the LLE in the reactor (Huxoll et al., 2022), no sudden drop in reaction yields was observed during the experiment, suggesting that the accumulated water did not cause formation of a biphasic mixture, which would have hindered the reaction. The miniplant was restarted with the input $\hat{\boldsymbol{u}}^0$, before turning on MAWQA with GMA again, to ensure that the process behaviour is not altered. After observing a similar performance, MAWQA with GMA was reactivated, and the experiment was continued.

Fig. 8 shows a surface plot that was fitted to the measured objective function values of the RA-process after completion of the experiment. Here no convexity condition was imposed. The plant-model mismatch is evident when compared to the surface plot of the adequate nominal model in Fig. 5. Nonetheless the optimum of both the nominal model and the identified convex QA model using process measurements both lie at a corner of the operating region. Although the nominal model did not capture the process accurately, it did capture the extreme point of the plant behaviour. This however was by no means clear before the experiment was performed due to the model errors and also the assumptions that entered into the model especially in the kinetics.

6. Discussion

The reductive amination reaction process to convert undecanal with DEA to an amine in a continuously operated miniplant was optimized during operation. The iterative real-time optimization method MAWQA with GMA was employed for the iterative optimization. An adequate nominal model was obtained by fitting a QA function to the nominal process model such that the Hessian of the model-based optimization

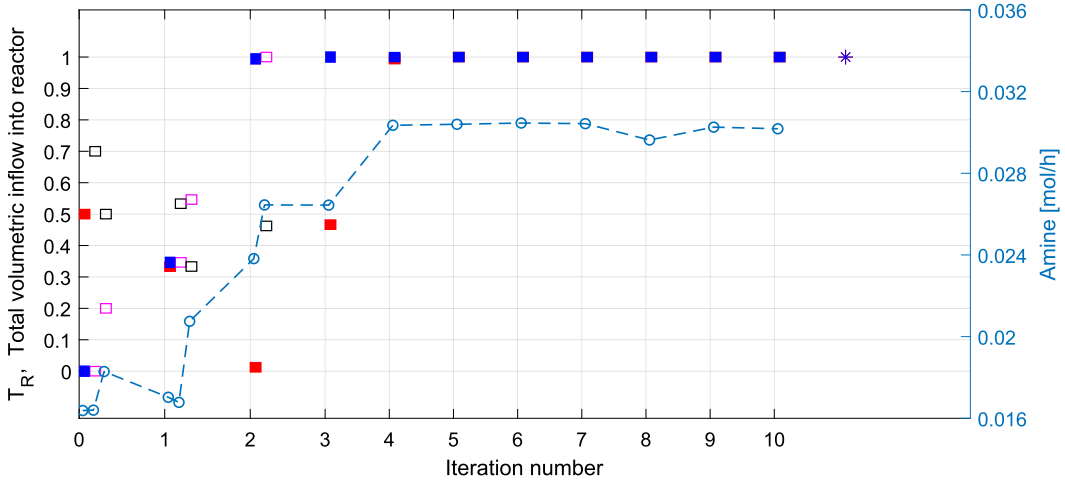

Fig. 6. Evolution of manipulated variables from $\hat{\boldsymbol{u}}^0$ to $\boldsymbol{u}_p^*$, computed by MAWQA with GMA, and the corresponding objective function values computed from real-process measurements. The inputs to the RA-process are represented by red and blue square–markers for u_1 and u_2. Additional process perturbations that were implemented to compute the process gradients are represented by black and magenta square–markers for u_1 and u_2. The objective function values are represented by blue circle–markers. Each vertical line represents an RTO iteration. Note that in one iteration, several inputs may have been applied because of the need for additional information from measurements.

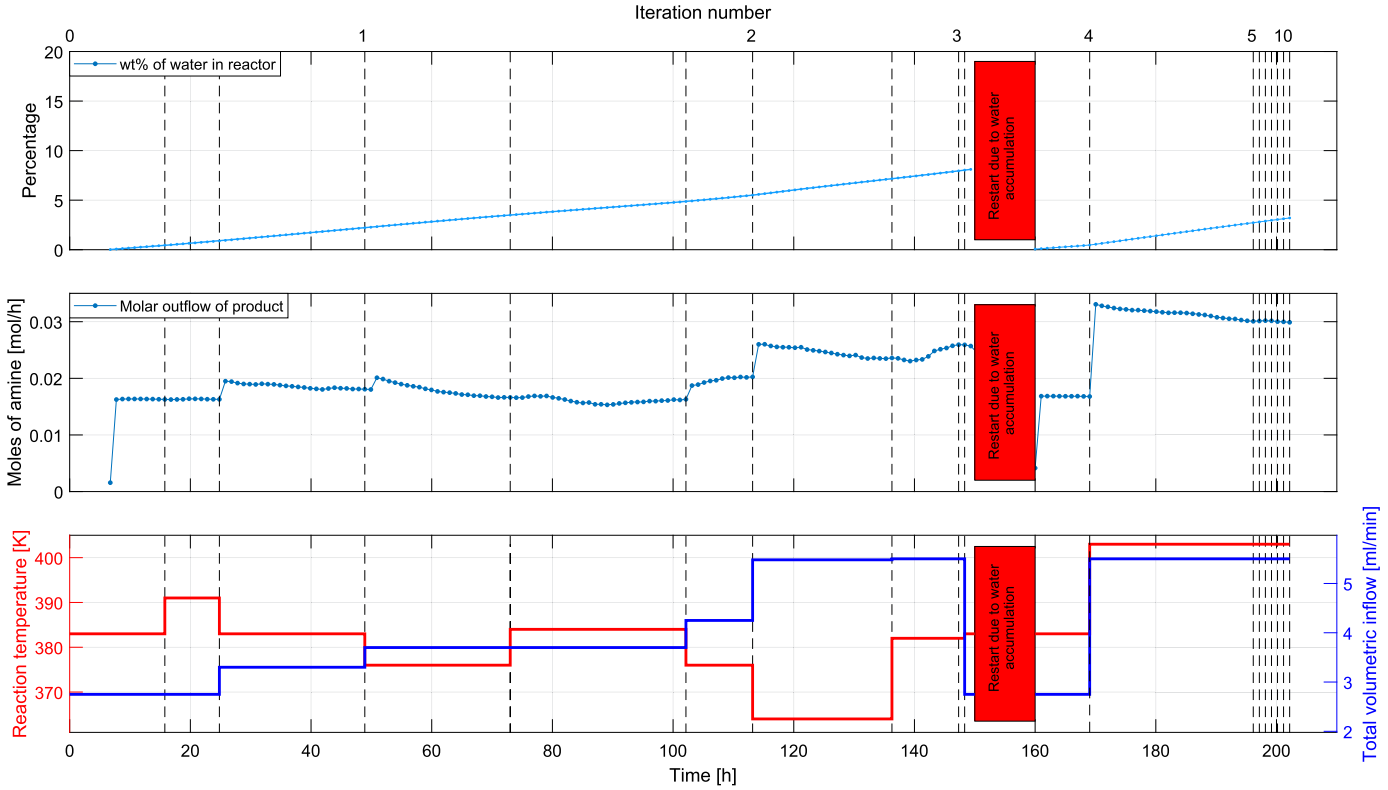

Fig. 7. Top figure: Weight percentage of water in the reactor computed using the experimental process measurements. Middle figure: Evolution of the objective function. Bottom Figure: Inputs to the RA-process. Each vertical dashed line represents a steady-state/new input.

problem is negative definite. Data reconciliation was used to reduce the effect of gross measurement errors and to ensure that the mass balances are satisfied. The plant-model mismatch and the additional uncertainty introduced by the QA were handled well by the iterative RTO method. It identified the optimal inputs that maximize the molar flowrate of amine in the product stream in only four iterations, corresponding to 9 input moves and then kept the process at the optimum without unnecessary moves.

This work illustrates that a chemical processes can be optimized already during the development phase despite the absence of a reliable rigorous process model. In this work, we used only steady-state measurements to compute the plant gradients and to adapt the optimization problem. Transitions between steady states in industrial processes are often slow, especially in processes with internal recycle streams. This limitation can be overcome by estimating the steady-state gradient (or the steady-state itself) during the transient phase. Gradient estimation can be formulated as a time-varying parameter estimation problem, allowing adaptive estimation methods such as recursive extended least-squares (RELS) (Navia et al., 2017) or normalized least mean square algorithm (NLMS) (Oliveira-Silva et al., 2023). Alternatively, system

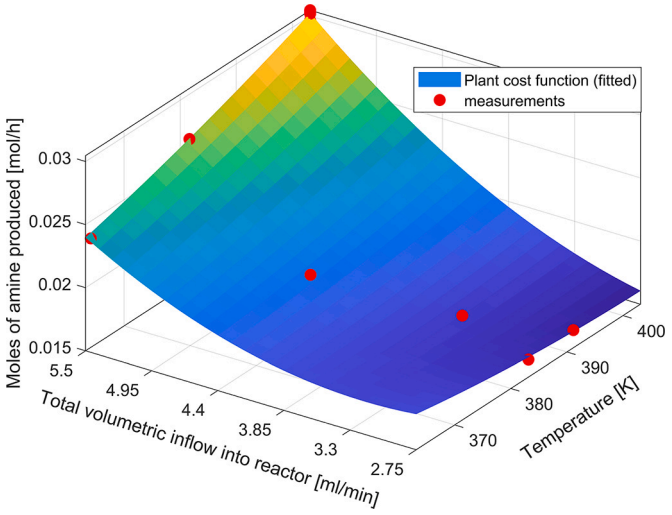

Fig. 8. Surface plot of the objective function $\dot{n}_{prod,Amine}$ fitted to the real process measurements.

identification methods may be used for steady-state estimation (Cadavid et al., 2017; Ferreira et al., 2017; Rodrigues et al., 2018; Rodríguez-Blanco et al., 2017; Speakman and François, 2020; François and Bonvin, 2014).

Abbreviations

The following abbreviations are used in this manuscript:

CO	Carbon monoxide
CSTR	Continuously stirred tank reactor
DEA	Diethylamine
GC	Gas chromatography
GMA	Guaranteed model adequacy
IGMO	Iterative gradient-modification optimization
ISOPE	Integrated system optimization and parameter estimation
LLE	Liquid–liquid equilibrium
MA	Modifier adaptation
MAWQA	Modifier adaptation with quadratic approximation
NLMS	Normalized least mean square algorithm
RELS	Recursive extended least-squares
PC-SAFT	Perturbed-chain statistical associating fluid theory
QA	Quadratic approximation
RA	Reductive amination
RTO	Real-time optimization
TMS	Thermomorphic multiphase system

CRediT authorship contribution statement

Conceptualization, Formal analysis, Methodology, Software, Investigation, Writing—original draft preparation, Validation, Visualization, A.R.G.M.; Conceptualization, Formal analysis, Investigation, Writing—original draft preparation, T.R.; Investigation, A.K.; Conceptualization, Funding acquisition, Supervision, Writing—review and detailed editing, D.V.; Conceptualization, Funding acquisition, Supervision, Writing—review and detailed editing, S.E. All authors have read and agreed to the published version of the manuscript.

Declaration of competing interest

The authors declare the following financial interests/personal relationships which may be considered as potential competing interests: Anwesh Reddy Gottu Mukkula reports financial support was provided by Deutsche Forschungsgemeinschaft. Tim Benjamin Riemer reports financial support was provided by Deutsche Forschungsgemeinschaft. Alexander Kuhl reports financial support was provided by Deutsche Forschungsgemeinschaft. Dieter Vogt reports financial support was provided by Deutsche Forschungsgemeinschaft. Sebastian Engell reports financial support was provided by Deutsche Forschungsgemeinschaft.

Data availability

No data was used for the research described in the article.

Acknowledgements

Gefördert durch die Deutsche Forschungsgemeinschaft (DFG)-TRR 63 “Integrierte chemische Prozesse in flüssigen Mehrphasensystemen” (Teilprojekt D4)-56091768 (supported by Deutsche Forschungsgemeinschaft in the context of the Interdisciplinary Research Centre TRR 63, Integrated Chemical Processes in Liquid Multiphase Systems, Subproject D4).

Appendix A. Mathematical model

The model equations are listed below:

1. Volume balance of the reactor:

$$\dot{V}_{in} = \dot{V}_{out} = \dot{V}_{feed} + \dot{V}_{recycle}, \tag{A.1a}$$

where $\dot{V}_{feed}, \dot{V}_{recycle}, \dot{V}_{in}$ and $\dot{V}_{out}$ are the volumetric flowrates of the fresh feed, recycle stream, reactor inlet and outlet stream respectively.

2. Molar balance of component i, in the liquid phase of the reactor n_i:

$$\frac{dn_i}{dt} = \dot{n}_{i,in} - \dot{n}_{i,out} + V_R r_i, \tag{A.2a}$$

$$\dot{n}_{i,in} = \dot{n}_{i,feed} + \dot{n}_{i,recycle}, \tag{A.2b}$$

$$\dot{n}_{i,out} = \frac{n_i \dot{V}_{out}}{V_R}, \tag{A.2c}$$

where $i \in \{$undecanal, DEA, aldol, alcohol, amine, enamine, H_2O, methanol, dodecane, $H_2\}$. V_R is the reactor volume and $\dot{n}_{i,in}, \dot{n}_{i,out}$ are the molar flowrates of component i into and out of the reactor. $\dot{n}_{i,feed}, \dot{n}_{i,recycle}$ are the molar flowrates of component i in the fresh feed and the recycle stream. The reaction rate r for each component is defined as (Kirschtowski et al., 2020):

$$r_{undecanal} = -r_{EC} - r_{HYDb} - r_{ADD}, \tag{A.3a}$$

$$r_{DEA} = -r_{EC} + r_{ADD}, \tag{A.3b}$$

$$r_{aldol} = r_{ADD}, \tag{A.3c}$$

$$r_{alcohol} = r_{HYDb}, \tag{A.3d}$$

$$r_{amine} = r_{HYDa}, \tag{A.3e}$$

$$r_{enamine} = r_{EC} - r_{HYDa} - r_{ADD}, \tag{A.3f}$$

$$r_{H_2O} = r_{EC}, \tag{A.3g}$$

$$r_{H_2} = \beta_{eff}\left(\frac{p^*_{H_2}}{H_{H_2}} - C_{H_2}\right) - r_{HYDa} - r_{HYDb}, \tag{A.3h}$$

$$r_{methanol} = 0, \tag{A.3i}$$

$$r_{dodecane} = 0, \tag{A.3j}$$

where H_{H_2}, β_{eff} are the Henry and mass transfer coefficients and $p^*_{H_2}, C_{H_2}$ represent the partial pressure due to H_2 and the concentration of H_2 in the liquid phase. The rate equations are defined as (Kirschtowski et al., 2020):

Table A.1
Parameters in the DAE model for RA reaction in the miniplant (Kirschtowski et al., 2020).

Parameter	Value	Units
$k_{EC,0}$	87.76	$L\,mol^{-1}\,min^{-1}$
$k_{HYDa,0}$	2.57×10^7	$L^2\,mol^{-1}\,min^{-1}$
$k_{HYDb,0}$	2.24×10^8	$L^2\,mol^{-1}\,min^{-1}$
$k_{ADD,0}$	1.40×10^5	$L\,mol^{-1}\,min^{-1}$
$\triangle E_{A,EC}$	13.9×10^3	$J\,mol^{-1}$
$\triangle E_{A,HYDa}$	19.4×10^3	$J\,mol^{-1}$
$\triangle E_{A,HYDb}$	44×10^3	$J\,mol^{-1}$
$\triangle E_{A,ADD}$	42.3×10^3	$J\,mol^{-1}$
R	8.3145	$J\,mol^{-1}\,K^{-1}$
H_{H_2}	3.44×10^2	$bar\,L\,mol^{-1}$
$\triangle G$	-8×10^3	$J\,mol^{-1}$
β_{eff}	2.07	min^{-1}
C_{H_2}	10	$mol\,L^{-1}$
$n_{catalyst}$	4.95×10^{-5}	$mol\,L^{-1}$

$$r_{EC} = \frac{k_{EC}}{{V_R}^2}\left(n_{undecanal} n_{DEA} - \frac{n_{enamine} n_{H_2O}}{k_{EQ}}\right), \tag{A.4a}$$

$$r_{HYDa} = \frac{k_{HYDa}}{{V_R}^3} n_{catalyst} n_{enamine} n_{H_2}, \tag{A.4b}$$

$$r_{HYDb} = \frac{k_{HYDb}}{{V_R}^3} n_{catalyst} n_{undecanal} n_{H_2}, \tag{A.4c}$$

$$r_{ADD} = \frac{k_{ADD}}{{V_R}^2} n_{undecanal} n_{enamine}, \tag{A.4d}$$

and the rate constants are defined by the Arrhenius equations:

$$k_j = k_{j,0} \exp\left(\frac{-\triangle E_{A,j}}{RT_R}\right) \quad \forall j \in \{EC, HYDa, HYDb, ADD\}, \tag{A.5a}$$

$$k_{EQ} = \exp\left(\frac{-\triangle G}{RT_R}\right). \tag{A.5b}$$

The values of the model parameters in the above equations are listed in Table A.1.

3. Volume balance of the decanter:

$$\dot{V}_{out} = \dot{V}_{product} + \dot{V}_{recycle}, \tag{A.6a}$$

where $\dot{V}_{product}$ is the volumetric flowrate of the product stream.

4. Molar balance of component i in the decanter:

$$\dot{n}_{i,product} = \zeta_i \dot{n}_{i,out}, \tag{A.7a}$$

$$\dot{n}_{i,recycle} = (1 - \zeta_i)\dot{n}_{i,out}, \tag{A.7b}$$

where $i \in \{$undecanal, DEA, aldol, alcohol, amine, enamine, H_2O, methanol, dodecane, $H_2\}$. $\dot{n}_{i,product}$ is the molar flowrate of component i in the product stream. The distribution coefficient ζ of component i in the decanter is predicted using surrogate models (Nentwich et al., 2019; Nentwich and Engell, 2019) of the PC-SAFT model for LLE reported in Huxoll et al. (2022).

References

Afanasyev, O.I., Kuchuk, E., Usanov, D.L., Chusov, D., 2019. Reductive amination in the synthesis of pharmaceuticals. Chem. Rev. 119 (23), 11857–11911.

Ahmad, A., Gao, W., Engell, S., 2019. A study of model adaptation in iterative real-time optimization of processes with uncertainties. Comput. Chem. Eng. 122, 218–227.

Bianga, J., Künnemann, K.U., Gaide, T., Vorholt, A.J., Seidensticker, T., Dreimann, J.M., Vogt, D., 2019. Thermomorphic multiphase systems: switchable solvent mixtures for the recovery of homogeneous catalysts in batch and flow processes. Chemistry 25 (50), 11586–11608.

Bianga, J., Kopplin, N., Hülsmann, J., Vogt, D., Seidensticker, T., 2020a. Rhodium-catalysed reductive amination for the synthesis of tertiary amines. Adv. Synth. Catal. 362 (20), 4415–4424.

Bianga, J., Künnemann, K.U., Goclik, L., Schurm, L., Vogt, D., Seidensticker, T., 2020b. Tandem catalytic amine synthesis from alkenes in continuous flow enabled by integrated catalyst recycling. ACS Catal. 10 (11), 6463–6472.

Bonvin, D., Srinivasan, B., 2013. On the role of the necessary conditions of optimality in structuring dynamic real-time optimization schemes. Comput. Chem. Eng. 51, 172–180.

Brdyś, M., Tatjewski, P., 2005. Iterative Algorithms for Multilayer Optimizing Control. World Scientific.

Cadavid, J., Hernández, R., Engell, S., 2017. Speed-up of iterative real-time optimization by estimating the steady states in the transient phase using nonlinear system identification, 20th IFAC World Congress. IFAC-PapersOnLine 50 (1), 11269–11274.

Chachuat, B., Srinivasan, B., Bonvin, D., 2008. Model parameterization tailored to real-time optimization. In: Braunschweig, B., Joulia, X. (Eds.), 18th European Symposium on Computer Aided Process Engineering. In: Computer Aided Chemical Engineering, vol. 25. Elsevier, pp. 1–13.

Chen, C.Y., Joseph, B., 1987. On-line optimization using a two-phase approach: an application study. Ind. Eng. Chem. Res. 26 (9), 1924–1930.

Darby, M.L., Nikolaou, M., Jones, J., Nicholson, D., 2011. Rto: an overview and assessment of current practice. J. Process Control 21 (6), 874–884.

Dennis Jr., J.E., Welsch, R.E., 1978. Techniques for nonlinear least squares and robust regression. Commun. Stat., Simul. Comput. 7 (4), 345–359.

Engell, S., 2007. Feedback control for optimal process operation. J. Process Control 17 (3), 203–219.

Engell, S., 2022. Introduction to chapter 5. In: Kraume, M., Enders, S., Drews, A., Schomäcker, R., Engell, S., Sundmacher, K. (Eds.), Integrated Chemical Processes in Liquid Multiphase Systems. De Gruyter, Berlin, Boston, pp. 361–508.

Faulwasser, T., Bonvin, D., 2014. On the use of second-order modifiers for real-time optimization. IFAC Proc. Vol. 47 (3), 7622–7628.

Ferreira, T.D.A., François, G., Marchetti, A.G., Bonvin, D., 2017. Use of transient measurements for static real-time optimization, 20th IFAC World Congress. IFAC-PapersOnLine 50 (1), 5737–5742.

Forbes, J., Marlin, T., 1996. Design cost: a systematic approach to technology selection for model-based real-time optimization systems. Comput. Chem. Eng. 20 (6), 717–734.

François, G., Bonvin, D., 2013. Use of convex model approximations for real-time optimization via modifier adaptation. Ind. Eng. Chem. Res. 52 (33), 11614–11625.

François, G., Bonvin, D., 2014. Use of transient measurements for the optimization of steady-state performance via modifier adaptation. Ind. Eng. Chem. Res. 53 (13), 5148–5159.

Gao, W., Engell, S., 2005. Iterative set-point optimization of batch chromatography. Comput. Chem. Eng. 29 (6), 1401–1409.

Gao, W., Wenzel, S., Engell, S., 2015. Integration of gradient adaptation and quadratic approximation in real-time optimization. In: 2015 34th Chinese Control Conference (CCC), pp. 2780–2785.

Gao, W., Wenzel, S., Engell, S., 2016. A reliable modifier-adaptation strategy for real-time optimization. Comput. Chem. Eng. 91, 318–328.

Gottu Mukkula, A.R., Engell, S., 2020. Guaranteed model adequacy for modifier adaptation with quadratic approximation. In: 2020 European Control Conference (ECC), pp. 1037–1042.

Gottu Mukkula, A.R., Kern, S., Salge, M., Holtkamp, M., Guhl, S., Fleicher, C., Meyer, K., Remelhe, M., Maiwald, M., Engell, S., 2020a. An application of modifier adaptation with quadratic approximation on a pilot scale plant in industrial environment, 21st IFAC World Congress. IFAC-PapersOnLine 53 (2), 11773–11779.

Gottu Mukkula, A.R., Valiauga, P., Fikar, M., Paulen, R., Engell, S., 2020b. Experimental real time optimization of a continuous membrane separation plant, 21st IFAC World Congress. IFAC-PapersOnLine 53 (2), 11786–11793.

Gürsel, I.V., Noël, T., Wang, Q., Hessel, V., 2015. Separation/recycling methods for homogeneous transition metal catalysts in continuous flow. Green Chem. 17 (4), 2012–2026.

Hahn, G., Kunnas, P., de Jonge, N., Kempe, R., 2019. General synthesis of primary amines via reductive amination employing a reusable nickel catalyst. Nat. Catal. 2 (1), 71–77.

Hayes, K., 2001. Industrial processes for manufacturing amines. In: Hoelderich Special Issue. Appl. Catal. A, Gen. 221 (1), 187–195.

Hernandez, R., Dreimann, J., Vorholt, A., Behr, A., Engell, S., 2018. Iterative real-time optimization scheme for optimal operation of chemical processes under uncertainty: proof of concept in a miniplant. Ind. Eng. Chem. Res. 57 (26), 8750–8770.

Huxoll, F., Kampwerth, A., Seidensticker, T., Vogt, D., Sadowski, G., 2022. Predicting solvent effects on homogeneity and kinetics of the hydroaminomethylation: a thermodynamic approach using pc-saft. Ind. Eng. Chem. Res. 61 (5), 2323–2332.

Jagadeesh, R.V., Murugesan, K., Alshammari, A.S., Neumann, H., Pohl, M.-M., Radnik, J., Beller, M., 2017. Mof-derived cobalt nanoparticles catalyze a general synthesis of amines. Science 358 (6361), 326–332.

Jameel, F., Stein, M., 2022. The many roles of solvent in homogeneous catalysis - the reductive amination showcase. J. Catal. 405, 24–34.

Jang, S.-S., Joseph, B., Mukai, H., 1987. On-line optimization of constrained multivariable chemical processes. AIChE J. 33 (1), 26–35.

Jäschke, J., Skogestad, S., 2011. Nco tracking and self-optimizing control in the context of real-time optimization. J. Process Control 21 (10), 1407–1416.

Kirschtowski, S., Kadar, C., Seidel-Morgenstern, A., Hamel, C., 2020. Kinetic modeling of rhodium-catalyzed reductive amination of undecanal in different solvent systems. Chem. Ing. Tech. 92 (5), 582–588.

Kirschtowski, S., Jameel, F., Stein, M., Seidel-Morgenstern, A., Hamel, C., 2021. Kinetics of the reductive amination of 1-undecanal in thermomorphic multicomponent system. Chem. Eng. Sci. 230, 116187.

Korpela, T., Suominen, O., Majanne, Y., Laukkanen, V., Lautala, P., 2016. Robust data reconciliation of combustion variables in multi-fuel fired industrial boilers. Control Eng. Pract. 55, 101–115.

Krstić, M., Wang, H.-H., 2000. Stability of extremum seeking feedback for general nonlinear dynamic systems. Automatica 36 (4), 595–601.

Künnemann, K.U., Bianga, J., Scheel, R., Seidensticker, T., Dreimann, J.M., Vogt, D., 2020. Process development for the rhodium-catalyzed reductive amination in a thermomorphic multiphase system. Org. Process Res. Dev. 24 (1), 41–49.

Marchetti, A., Chachuat, B., Bonvin, D., 2009. Modifier-adaptation methodology for real-time optimization. Ind. Eng. Chem. Res. 48 (13), 6022–6033.

Marchetti, A.G., François, G., Faulwasser, T., Bonvin, D., 2016. Modifier adaptation for real-time optimization–methods and applications. Processes 4 (4), 55.

Marchetti, A.G., de Avila Ferreira, T., Costello, S., Bonvin, D., 2020. Modifier adaptation as a feedback control scheme. Ind. Eng. Chem. Res. 59 (6), 2261–2274.

Mignonac, G., 1921. Nouvelle méthode générale de préparation des amines à partir des aldéhydes ou des cétones. C. R. 172, 223–225.

Navia, D., Puen, A., Bergh, L., Rodriguez-Blanco, T., Sarabia, D., de Prada, C., 2017. Modifier-adaptation based on transient measurements applied to a laboratory-scale flotation column. In: Espuña, A., Graells, M., Puigjaner, L. (Eds.), 27th European Symposium on Computer Aided Process Engineering. In: Computer Aided Chemical Engineering, vol. 40. Elsevier, pp. 1729–1734.

Nentwich, C., Engell, S., 2019. Surrogate modeling of phase equilibrium calculations using adaptive sampling. Comput. Chem. Eng. 126, 204–217.

Nentwich, C., Winz, J., Engell, S., 2019. Surrogate modeling of fugacity coefficients using adaptive sampling. Ind. Eng. Chem. Res. 58 (40), 18703–18716.

Oliveira-Silva, E., de Prada, C., Montes, D., Navia, D., 2023. Economic mpc with modifier adaptation using transient measurements. Comput. Chem. Eng. 173, 108205.

Reshi, N.U.D., Saptal, V.B., Beller, M., Bera, J.K., 2021. Recent progress in transition-metal-catalyzed asymmetric reductive amination. ACS Catal. 11 (22), 13809–13837.

Roberts, P., 1979. An algorithm for steady-state system optimization and parameter estimation. Int. J. Syst. Sci. 10 (7), 719–734.

Roberts, P., 2000. Broyden derivative approximation in isope optimising and optimal control algorithms. IFAC Proc. Vol. 33 (16), 293–298.

Rodrigues, D., Amrhein, M., Billeter, J., Bonvin, D., 2018. Fast estimation of plant steady state for imperfectly known dynamic systems, with application to real-time optimization. Ind. Eng. Chem. Res. 57 (10), 3699–3716.

Rodríguez-Blanco, T., Sarabia, D., Pitarch, J., de Prada, C., 2017. Modifier adaptation methodology based on transient and static measurements for RTO to cope with structural uncertainty. Comput. Chem. Eng. 106, 480–500.

Rosen, J.B., Marcia, R.F., 2004. Convex quadratic approximation. Comput. Optim. Appl. 28, 173–184.

Schlüter, S., Künnemann, K.U., Freis, M., Roth, T., Vogt, D., Dreimann, J.M., Skiborowski, M., 2021. Continuous co-product separation by organic solvent nanofiltration for the hydroaminomethylation in a thermomorphic multiphase system. Chem. Eng. J. 409, 128219.

Speakman, J., François, G., 2020. Real-time optimization via modifier adaptation of closed-loop processes using transient measurements. Comput. Chem. Eng. 140, 106969.

Strohmann, M., Vorholt, A.J., Leitner, W., 2022. Branched tertiary amines from aldehydes and α-olefins by combined multiphase tandem reactions. Chemistry 28 (58), e202202081.

Tatjewski, P., 2002. Iterative optimizing set-point control–the basic principle redesigned. IFAC Proc. Vol. 35 (1), 49–54.

Weber, A., Porthun, L., Schomäcker, R., 2021. Rh-catalyzed reductive amination of undecanal in an aqueous microemulsion system using a non-ionic surfactant. Catalysts 11 (10), 1223.

Wenzel, S., Gao, W., Engell, S., 2015. Handling disturbances in modifier adaptation with quadratic approximation. IFAC-PapersOnLine 48, 132–137.

Wenzel, S., Yfantis, V., Gao, W., 2017. Comparison of regression data selection strategies for quadratic approximation in RTO. In: Computer Aided Chemical Engineering, vol. 40, pp. 1711–1716.